POROSITY EVOLUTION IN ALUMINUM ALLOY 2024 BOP AND BUTT DEFOCUSED WELDING BY YB-YAG DISK LASER

Vittorio ALFIERI – Francesco CARDAROPOLI – Fabrizia CAIAZZO – Vincenzo SERGI

Abstract: *In many industrial applications, in order to obtain good results in laser welding processes, it may not be sufficient to use a focused beam on the upper surface, so a defocused beam is required instead. This study aims to investigate which advantages a defocused beam may offer in welding aluminum alloy 2024 using Yb:YAG disk laser. A characterization of laser beam geometry is preliminary necessary, in order to correlate bead features and effective specific energy provided. Porosity content decrease and enhanced penetration depth have been obtained with defocused beam; welding behavior has been related to magnesium loss via EDS analysis. Considering the shape of the cross sections of the bead in butt welding, the relation between key-hole instability and porosity formation has also been discussed. For the alloy in exam, the welding range to perform structurally sound and defect-free welds is found to be tight.*

Keywords:
 – laser welding
 – aluminum alloy
 – defocusing
 – porosity
 – disk laser

1. INTRODUCTION

Porosity development is one of the main issues in laser welding processes of aluminum alloys. Many studies have pointed out that two kinds of porosity arise. Micro porosities, whose mean diameter ranges between 50 and 200 µm [1] normally do not result in the rejection of welded parts: they are ascribed to hydrogen and other common gases which are released and trapped in the solidifying alloy as their solubility in liquid metal is much higher compared to that one in solid state [2, 3]. Macro porosities, instead, whose size ranges between 300 and 600 µm, seriously affect mechanical properties of the welding bead and are due to imperfect collapses of the key-hole during welding and are common in aluminum alloys as high Mg content favors gas occlusions and non-stable key-holes [1].

Macro porosity evolution depends on welding conditions. Previous studies [4] have proved that a significant influence is due to the thermal input, which is in direct ratio to power level and in inverse ratio to scan speed. Higher thermal inputs are beneficial in full penetrative beads, whereas lower thermal input reduces vaporization and instability-inducted pores formation in incomplete penetrative welds. There are suggestions that welding in defocused conditions may also result in lower porosity content or enhanced penetration depth [5, 6]. This behavior has also been noticed for aluminum alloys [1, 3]. Laser beam, indeed, presents a convergent geometry towards the waist, where the radius has a minimum; then it diverges again, with symmetrical trend. When welding in defocusing conditions, the beam focus point locates inside or outside the upper surface, so that material response is different due to the variation of the spot size compared to the focused spot.

Conventionally, both positive and negative defocusing designate conditions in which the focal point is placed respectively above and below the top surface of the workpiece. In both cases, specific energy provided and fused zone extent change. Therefore, penetration depth is different. When processing parameters are quite close to the threshold value to melt the alloy, too much high defocusing values do not allow starting a key-hole

mode. Conversely, once the specific energy is adequate, the liquid surface is depressed by the recoil force of evaporation: for positive defocusing the beam is divergent and the depression moves the liquid surface away from the focal point; as a result, the specific energy decreases along the thickness of the piece. For negative defocusing, instead, the beam is convergent and the depression of the liquid surface exposes the bottom surface to a higher specific energy, so once a key-hole is produced, it has a tendency to further grow into a deeper one [3].

2. BEAM CHARACTERISATION

The defocusing range usually is in the order of few millimeters, where geometric features of the beam allow obtaining a significant variation of the spot diameter. A preliminary analysis of the beam is therefore necessary in order to determine the variation of beam radius along the propagation axis and to further calculate values of specific energy effectively provided [6, 7].

The "Rayleigh length" z_R of a laser beam is the distance from the beam waist where the beam diameter d is increased by a factor of the square root of 2, so that the spot area is double compared to the focused one where diameter has its minimum d_0. According to the wave propagation equation, being z the distance from the focal point and θ the divergence of the laser beam, diameter variation along the propagation axis is expressed by:

$$d^2(z) = d_0^2 + z^2\theta^2 \qquad (1)$$

for small divergence angle, in the order of tenths of a radiant, as in the case of industrial laser beams. The divergence angle is measured between the hyperbola asymptotes, which give an approximation of the beam profile in the far field, away from the beam waist. Small divergent beams are therefore characterized by a small variation of the spot diameter along the propagation axis. The Rayleigh length, from the equation (1), is:

$$z_R = \frac{d_0}{\theta} \qquad (2)$$

Therefore, diameter variation is also expressed by:

$$d(z) = d_0\sqrt{1+\left(\frac{z}{z_R}\right)^2} \qquad (3)$$

Higher depth of focus are required so that the beam diameter remains constant, within certain limits, to provide uniform irradiance through the workpiece thickness, in cutting or deep welding applications. In the tests, a Trumpf TruDisk 2002 Yb:YAG disk laser, 2 kW max power level, emitting at 1030 nm, has been used to prepare the samples. Technical data of the welding system, which consists of a 6-axis robot and optics, are listed in Table 1.

Table 1.   Welding system technical data

Maximum output power [kW]	2.0
Laser light wavelength [nm]	1030
Beam Parameter Product [mm × mrad]	8.0
Focus diameter [μm]	300
Focal length [mm]	200
Maximum power density [kW/mm^2]	28.3

Using a focal length of 200 mm, the minimum diameter is of 0.300 mm. Considering the Beam Parameter Product value, which is the product between beam radius, measured at the beam waist, and the beam divergence half-angle, measured in the far field, a 106.7 mrad divergence angle value is obtained. The Rayleigh length is therefore of 2.81 mm. The beam geometry is shown in Figure 1.
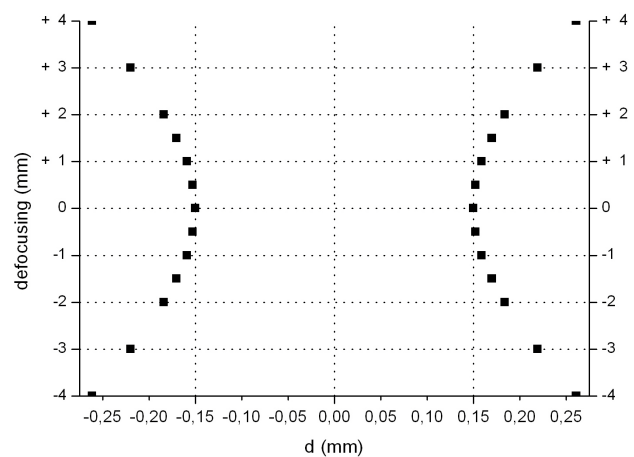

Figure 1. Beam geometry

3. EXPERIMENTAL PROCEDURE

In order to carry out rigorous tests, a preliminary procedure to find the focus point is required. On the upper surface of an anodized aluminum sheet, several welding points have been performed, changing the distance between the laser head and the sheet. Each point has been spotted using a 300 W single rectangular pulse input, for a 50 ms time, thus producing vaporisation on the upper layer of the sheet. The spots have been measured via optical microscopy. The focus point is exactly on the surface of the sheet when the spot has minimum diameter. This procedure defines the focal position to further defocus the beam around. Tests have been carried out on AA 2024-T3, which is largely used in industry, mainly automotive, aeronautic and military [8], although seriously susceptible to porosity formation. Nominal composition of the alloy is listed in Table 2.

Table 2. Chemical composition of AA 2024 (wt.%)

Cu	Mg	Mn	Si
3.80 ÷ 4.90	1.20 ÷ 1.80	0.30 ÷ 0.90	0.50

Fe	Zn	Ti	Cr	Al
0.50	0.25	0.15	0.1	Bal.

Bead-on-plate (BOP) and butt autogenous welds have been produced in continuous wave mode on 3.2 mm thick plates; helium has been adopted as shielding gas with a flow rate of 30 l/min opposite to the welding direction which, according to set-up experiments, allows to obtain better shielding compared to a forward flow rate. The angle between the nozzle axis and the workpiece is 25°. A high speed compressed air cross-jet has been used to protect the optics from possible molten metal spatters which are quite common in laser welding. Additionally, the laser beam angle is 5°, to prevent damage to the optics due to back reflection, prompted by low aluminum absorptance.
The movement of laser beam is obtained through the robot ABB IRB 240 M2004 and sheets to be butt welded are tightened up together on the workbench using low height clamping jaws ensuring in this way that there is no gap between the plates. The experimental setup is shown in Figure 2. Preliminary procedures are needed before welding: a hydrofluoric and nitric acid mixture has been used as pickling agent to remove any oxide and lubricant

which may dissolve in the molten metal thus producing undesirable inclusions; then specimens have been further degreased with acetone just before welding. In addition, before starting each test, a welding point has been spotted at the beginning of the welding path, using a 180 J single rectangular pulse input: it has been found in previous works [9, 10] that this spot plays a major role as it locally reduces the reflectivity of aluminum in order to start a key-hole mode and enhance a deep penetration welding. In butt welding tests, an additional welding point has been spotted at the end of the welding path: in this way, welding points are also enhancing the tightening of the sheets.
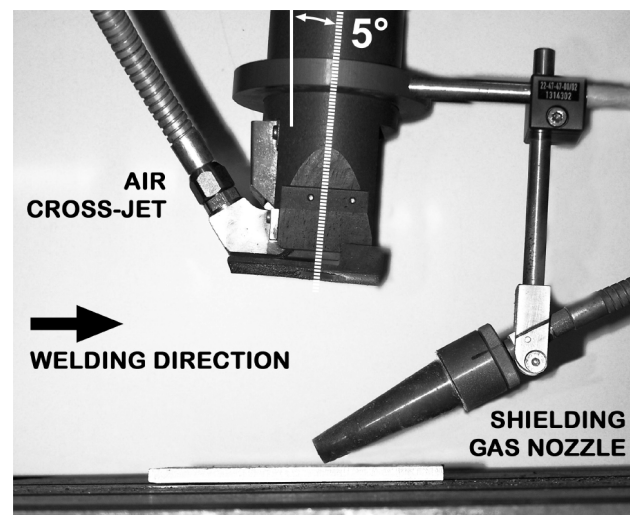

Figure 2. Experimental setup

A random test procedure has been arranged to produce the specimens, each one tripled to assure the reproducibility and obtain reliable data.
Welded BOP and butt samples have been cut using a Buehler abrasive cutter and then polished with SiC paper up to 800 grit. Chemical etching has been carried out using Keller's solution [11] at room temperature in order to highlight the bead boundaries in the section. For each operational condition, average welding depth, fused zone and porosity extent on longitudinal section have been evaluated via computer image tools. A 4 mm long zone both at the beginning and at the end of the bead has been excluded from measures in order to neglect any transitory effect due to key-hole opening and closure.
Transversal BOP cross sections have also been examined using a LEO EVO 50, with LaB6 gun SEM and resolution of 4 nm at 30 keV, equipped

with an energy dispersive spectrometer (EDS), Oxford INCA Energy 300; the available EDS detector can provide information starting from elements with atomic number higher than 4; the analyses have been performed operating at 20 keV primary energy with a probe current of 100 pA.

Transversal butt cross sections have been examined and related to key-hole stability, aiming to find out an operating window to perform welding without inducing any instability.

4. BOP TESTS

In order to discuss the effect of a defocused beam, power level and welding rate have been chosen and held in BOP tests: 1.6 kW power and 10 mm/s welding speed have been used as they guarantee full penetrative welding condition on 3.2 mm thick samples, with a significant porosity content (around 5% on average) whose behavior is easier to be monitored and, then, optimized. The effects of different focal positions have therefore been studied. To choose the defocusing range, the beam profile has to be considered. As observed before, with defocused laser beam welding, the power density on the top surface is lower compared to the value obtained in focused conditions, so less concentrated energy is transferred to the alloy. Previous tests [4] have shown that a specific power density of 18.4 kW/mm^2 has to be provided in order to sufficiently melt the surface and start a key-hole mode welding on the alloy in exam. Therefore, being the current test carried out using 1.6 kW power, sensible defocusing values should range from -1 to 1 mm. Power density (P_d) values for a given defocusing value are listed in Table 3, being z the distance from the focal point and $d(z)$ the spot diameter.

Table 3. Power density as a function of focus position

z [mm]	$d(z)$ [mm]	P_d [kW/ mm^2]
0	0.300	22.60
± 0.5	0.305	21.90
± 1.0	0.318	20.15
± 1.5	0.340	17.60

Penetration depth and porosity content as function of focus position are shown in Figure 3. Fusion develops when defocusing to 1 mm, both positive

and negative, as 20 kW/mm^2 specific power density are provided. Nevertheless, the welding behaviour is different when defocusing positive or negative: indeed, once the threshold value has been provided, a key-hole mode develops with negative defocusing, as the focal position locates within the material; conversely, a 1 mm positive defocusing melts the surface but is not adequate to start a key-hole mode as the beam expands through the material and although disk laser divergence is low, specific energy decreases along the propagation axis. It is inferred that even if the laser beam is symmetrical around the beam waist and along the propagation direction, different responses from the material are achieved with positive and negative defocusing, so the welding behaviour, in terms of penetration depth, is not symmetrical around the focus position. This assumption is also confirmed considering a comparison between samples obtained by defocusing at 0.5 mm, positive and negative. Providing the same specific energy on the upper surface, only the sample produced in negative defocusing conditions shows a deep penetrated bead. Nevertheless, both for positive and negative defocusing, but for different reasons, a reduction in porosity content is detected compared to the sample obtained focusing the beam on the surface of the material. Figure 4 shows the longitudinal sections of the sample obtained using a focused beam (up); the porosity content drops when defocusing to -1 mm (down).
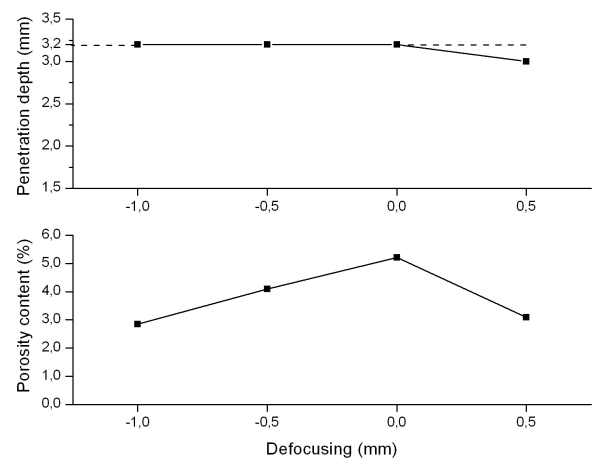

Figure 3. Penetration depth and porosity content as function of focus position

With positive defocusing, one should assume that the effect of the reduction in specific energy along the workpiece thickness produces lower average
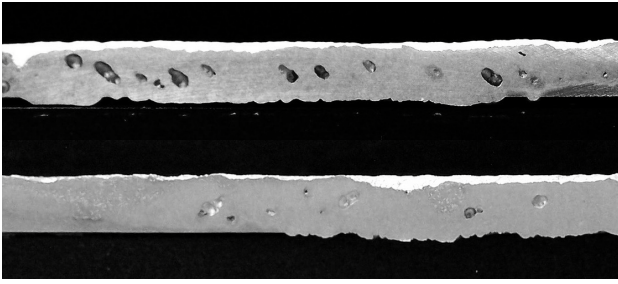
Figure 4. Longitudinal sections of the specimens obtained with focused beam (up) and defocusing to -1 mm (down)

Figure 5. Sites of interest on the cross section of a sample obtained with a -0.5 mm defocused beam

temperature in the melted pool; as a consequence, Mg loss through vaporisation decreases, so the key-hole is much more stable and instability-inducted macro porosities are reduced. For negative defocusing, instead, an explanation of the results is linked to melted material flow vortex structure in the melted pool when a key-hole welding condition is produced [6].

The increase in specific energy along the workpiece thickness is thought to enhance Mg expulsion. EDS analysis have been carried out to check the chemical concentration in the transverse cross section.

First of all, Mg content in the base material has been measured: the average value has been found to be of 1.56% and has been considered as the reference value to compare Mg percentage in the welded samples cross sections.

For each transverse cross section the chemical concentration has been evaluated in three sites of interest: the first one is completely in the fused zone; the second and the third areas are on the boundaries between the fused zone and heat affected one. An example of the position of the sites of interest is shown in Figure 5, with reference to BOP cross section of the sample obtained defocusing at -0.5 mm, also characterized by the presence of macroporosities.

Loss of Mg content has been found in each sample, in the fused zone and at the boundary of the heat affected zone. In the specimens, Mg concentration in the bulk of the weld metal, examined in site 1, is quite uniform, indicating that vigorous convective mixing occurred in the molten metal.
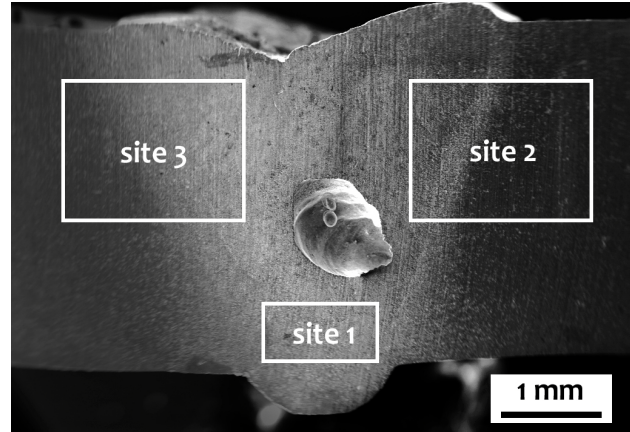
Reduction in Mg content has resulted in bubble formation and key-hole instability. Mg ejection is favoured using a negatively defocused beam as the average concentration value for Mg in the cross section drops, as an example, to 0.74% for the sample obtained defocusing to -0.5 mm.

In order to discuss the trend of magnesium concentration, results on site 3 are shown. Figure 6 shows analysis strategy: three scanning lines, each one composed by 5 points, have been considered at different depths. Mg content along the scanning lines is presented in Figure 7.
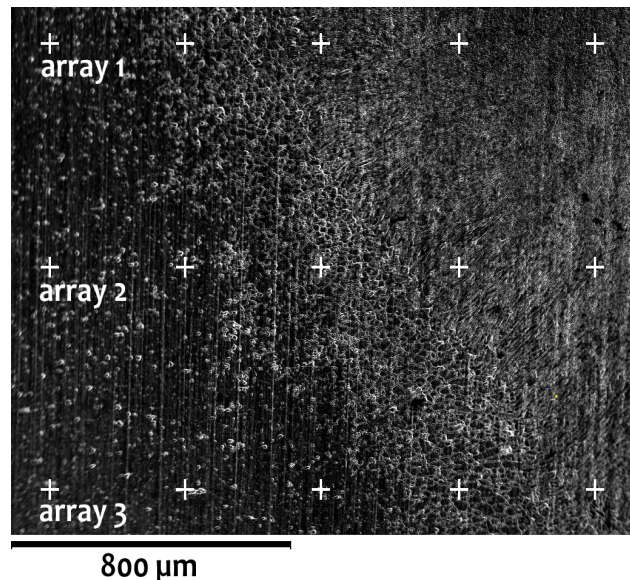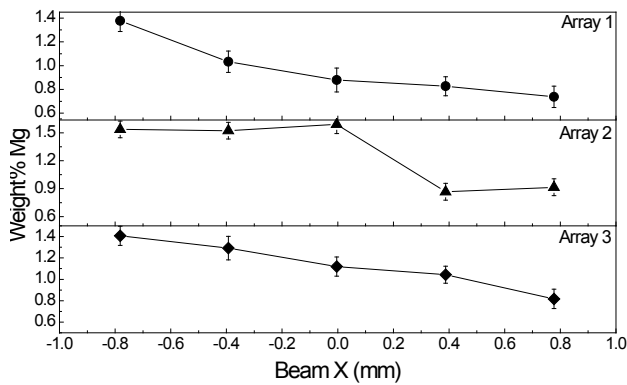

Figure 6. Analysis strategy

Figure 7. Mg content along the scanning lines

From the results obtained in site 2 and 3, it is possible to point out that Mg concentration decreases moving from the base material towards the melted zone.

Furthermore, a great variability in Cu content is apparent both in fused zone and heat affected zone. This behaviour is not univocal and probably connected with Cu tendency to segregate in intermetallic compound form at grain boundaries in the heat affected zone, and at dendrite structure in the fused zone. As a consequence, Cu content depends on the position of the scanning beam [12].

5. BUTT WELDING

Butt welding tests have been performed at 1.8 kW power level, with the same welding speed and defocusing range used in BOP tests. Thus, a higher thermal input has been produced since in deep penetrative welds higher thermal inputs are beneficial for the reduction of porosity content [4]. Penetration depth and porosity content as function of focus position are shown in Figure 8.

As expected, in focused condition porosity content decreases compared to BOP tests. Nevertheless, the increase in porosity content in some operative conditions has to be discussed. Different porosity shapes are shown in Figure 9: when produced, porosities in focused condition have roughly circular shape; whilst when defocusing to -1 mm, irregular shaped porosities are produced along the bead.

Porosity content detected when positive defocusing to 0.5 mm is due to incomplete penetration, as vapour expulsion is not complete, since the vortex structure of the melted zone does not reach the lower surface.
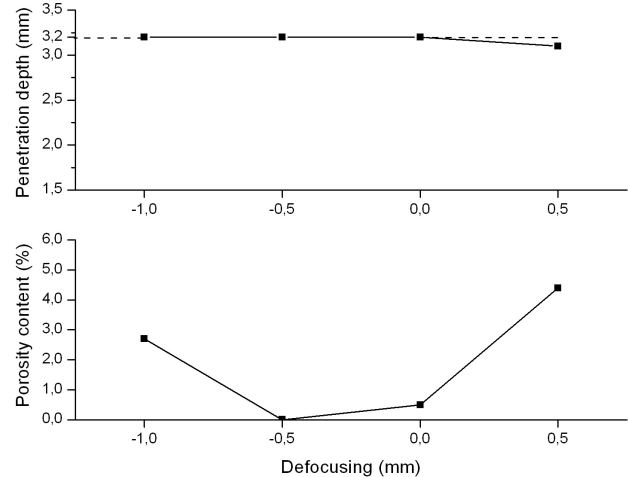

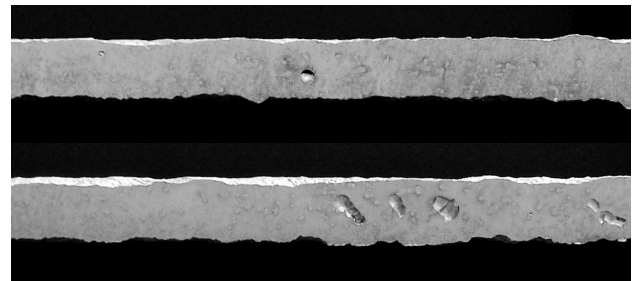*Figure 8. Penetration depth and porosity content as function of focus position*

Figure 9. Longitudinal sections of the butt-welded specimens obtained with focused beam (up) and defocusing to -1 mm (down)

Reasons for the increase in porosity content detected when defocusing to -1 mm has to be discussed referring to remarkable key-hole instability. In order to relate porosity formation and key-hole instability, transversal cross sections of the specimens are shown in Figure 10. Transversal cuts have been performed with a 10 mm step.

When defocusing to -1 mm, the bead shape is irregular along the welding direction, this proving that the test has been carried out in instability, which has resulted in porosity increase.

It is inferred that, compared to BOP tests, the interface between the plates and the different power level delivered in butt welding tests, affect the pressure terms in the balance, moving the stable solution for the equilibrium radius of the key-hole [13], so that the optimum welding range changes on a case-by-case basis and, for the aluminum alloy in exam, is highly susceptible to minimal deviations from the focal position.

Focus position: -1 mm | Focus position: -0.5 mm | Focus position: 0
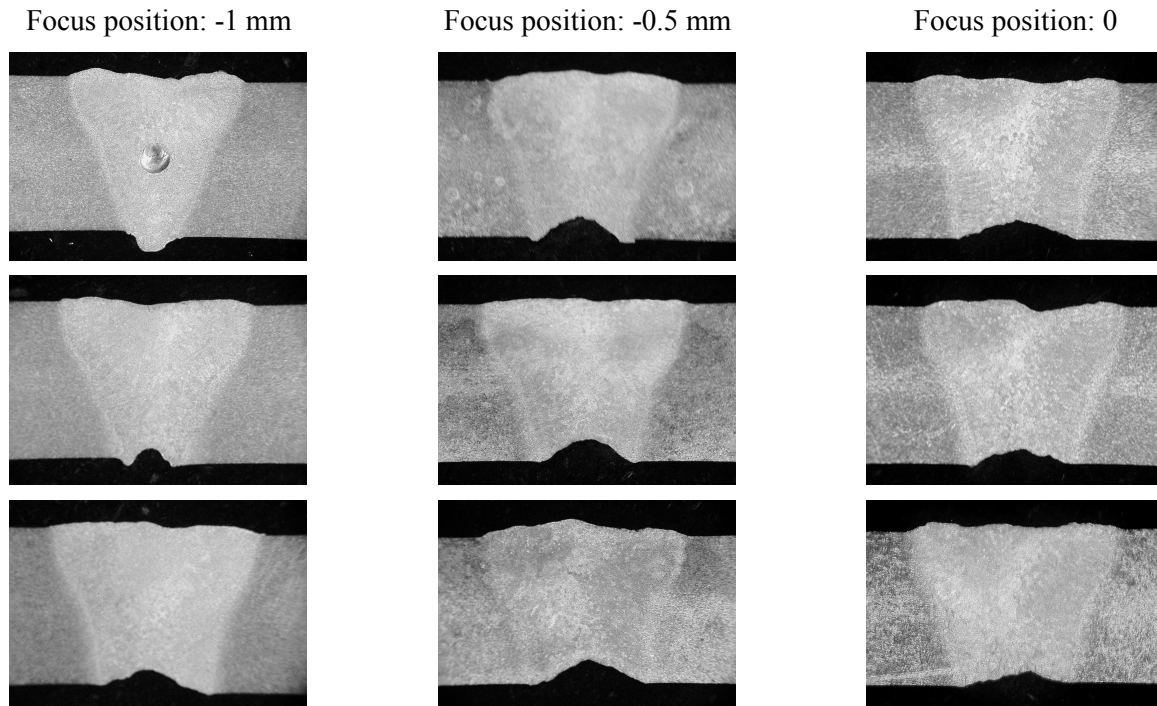

Figure 10. From left to right, cross sections of the butt welded specimens obtained with focus position to -1, -0.5 and 0 respectively; sections listed from up to down following the welding direction

6. CONCLUSION

The beam geometry has been evaluated in order to determine the effective values of specific energy provided during BOP and butt welding of AA 2024. The Rayleigh length for the welding system has been calculated, and then sensible defocusing values have been chosen to further carry out the tests. Porosity content decrease and enhanced penetration depth have been found for BOP specimens obtained with negative defocused beam, compared to those ones produced by focusing the beam on the upper surface of the material. Welding bead features have been related to specific energy trend along the workpiece thickness and to Mg loss. EDS analysis have proved that Mg content decreases in the molten area and is therefore responsible for key-hole instability which induces macro porosity formation in the bead.

Butt welds have, therefore, been performed, increasing the thermal input, in order to reduce the porosity content. When defocusing to 0.5 mm, the porosity content increases in comparison with focused welding. Considering the shape of the cross sections of the bead, the relation between key-hole instability and porosity formation has also been discussed. For the alloy in exam, the welding range is found to be tight to perform structurally sound and defect-free welds.

ACKNOWLEDGEMENTS

REFERENCES

[1] Haboudou, A., Peyre, P., Vannes, A. B., Peix, G.: *Reduction of porosity content generated during Nd: YAG laser welding of A356 and AA5083 aluminium alloys*, Materials Science and Engineering A, Vol. 363 (2003), p. 40-52

[2] Zhao, H., Debroy, T.: *Macroporosity free aluminum alloy weldments through numerical simulation of keyhole mode laser welding*, Journal of Applied Physics, Vol. 93 (2003), No. 12, p. 10089 – 10096

[3] Pastor, M., Zhao, H., Martukanitz, R. P., Debroy, T.: *Porosity, underfill and magnesium loss during continuous wave Nd:YAG laser welding of thin plates of aluminum alloys 5182*

and 5754, Welding Journal, Vol. 78 (1999), No. 12, p. 207-216

[4]   Alfieri, V., Cardaropoli, F., Caiazzo, F., Sergi, V.: *Investigation on porosity content in 2024 aluminum alloy welding by Yb:YAG disk laser*, Proceedings of 2011 International Conference on Manufacturing Science and Technology, Singapore, 2011, pp. 1-6

[5]   Duley, W. W.: *Laser Welding*, John Wiley and Sons Inc., New York, 1999

[6]   Steen, W. M.: *Laser Material Processing*, Springer, London, 2003

[7]   Capello, E.: *Le lavorazioni industriali mediante laser di potenza*, Maggioli Editore, Bologna, 2008

[8]   Ludovico, A. D., Daurelio, G., De Filippis, L.A.C., Scialpi, A., Squeo, F.: *Laser welding of the AA 2024-T3 aluminium alloy by using two different laser sources*, Proceedings of XV International Symposium on Gas Flow, Chemical Lasers and High Power Lasers, SPIE, Vol. 5777, 2005, pp. 887-894

[9]   Cardaropoli, F., Alfieri, V., Caiazzo, F., Sergi, V.: *Laser welding of aluminum alloy AA 2024 by Yb-YAG disk laser*, Proceedings of X AITeM Conference, Enhancing the Science of Manufacturing, Naples, Italy, 2011, pp. 1-16

[10] Alfieri, V., Cardaropoli, F., Caiazzo, F., Sergi, V.: *Effect of defocusing on porosity content evolution in aluminum alloy 2024 welding by Yb-YAG disk laser*, Proceedings of International Conference on Innovative Technologies IN-TECH, Bratislava, Slovakia, 2011, pp. 671-674

[11] *Aluminum and aluminum alloys*, ASM International, Davis ed., USA, 1993

[12] Wanjara, P., Brochu, M.: *Characterization of electron beam welded AA2024*, Vacuum, Vol. 85 (2010), p.268-282

[13] Klein, T., Vicanek, M., Kroos, J., Decker, I., Simon, G.: *Oscillations of the keyhole in penetration laser beam welding*, Journal of Physics D: Applied Physics, Vol. 27 (1994), No. 10, p. 2023 – 2030

Vittorio Alfieri
Francesco Cardaropoli
Fabrizia Caiazzo
Vincenzo Sergi
Dept. of Industrial Engineering, University of Salerno
Via Ponte Don Melillo
84084, Fisciano
Italy
valfieri@unisa.it
fcardaro@unisa.it
f.caiazzo@unisa.it
sergi@unisa.it